Role of the Distal Phenylalanine 54 on the Structure, Stability, and Ligand Binding of *Coprinus cinereus* Peroxidase†

Francesca Neri,‡ Chiara Indiani,‡ Beatrice Baldi,‡ Jesper Vind,§,|| Karen G. Welinder,§,⊥ and Giulietta Smulevich*,‡

Dipartimento di Chimica, Universita' di Firenze, Via G. Capponi 9, I-50121 Firenze, Italy, Department of Protein Chemistry, University of Copenhagen, Copenhagen, Denmark, Novo Nordisk A/S, Bagsværd, Denmark, and Biotechnology Laboratory, Aalborg University, Sohngaardsholmvej 57, DK-9000 Aalborg, Denmark

Received November 30, 1998; Revised Manuscript Received March 23, 1999

ABSTRACT: Resonance Raman and electronic absorption spectra obtained at various pH values for the Fe^{3+} form of distal F54 mutants of *Coprinus cinereus* peroxidase are reported, together with the Fe^{2+} form and fluoride and imidazole adducts at pH 6.0, 5.0, and 10.5, respectively. The distal phenylalanine residue has been replaced by the small aliphatic residues glycine and valine and the hydrogen-bonding aromatic residues tyrosine and tryptophan (F54G, -V, -Y, and -W, respectively). These mutations resulted in transitions between ferric high-spin five-coordinate and six-coordinate forms, and caused a decrease of the pK_a of the alkaline transition together with a higher tendency for unfolding. The mutations also alter the ability of the proteins to bind fluoride in such a way that those that are six-coordinate at pH 5.0 bind more strongly than both wild-type CIP and F54Y which are five-coordinate at this pH value. The data provide evidence that the architecture of the distal pocket of CIP is altered by the mutations. Direct evidence is provided that the distal phenylalanine plays an important role in controlling the conjugation between the vinyl double bonds and the porphyrin macrocycle, as indicated by the reorientation of the vinyl groups upon mutation of phenylalanine with the small aliphatic side chains of glycine and valine residues. Furthermore, it appears that the presence of the hydrogen-bonding tyrosine or tryptophan in the cavity increases the pK_a of the distal histidine for protonation compared with that of wild-type CIP.

The heme-containing peroxidases are divided into three classes depending on their amino acid sequence similarity. The three classes conserve key residues in the heme pocket, which are important for the enzymatic activity. In particular, the distal histidine and arginine residues and the proximal histidine, which is coordinated to the heme iron and hydrogen-bonded to an oxygen atom of the carboxylate group of an aspartic acid, are conserved. The three classes also have a conserved aromatic side chain on the distal side of the heme. This is an indole group in class I peroxidases [W51 in mitochondrial cytochrome *c* peroxidase (CCP)[1] and W41 in the majority of the intracellular ascorbate peroxidases (APX)] and a phenyl group in class II [F54 in *Coprinus cinereus* peroxidase (CIP), F46 in lignin peroxidase (LIP), and F45 in manganese peroxidase (MnP)] and class III peroxidases [F41 in horseradish peroxidase isozyme C (HRP-C)]. Interestingly, two novel types of intracellular ascorbate peroxidases also contain a distal phenylalanine rather than the tryptophan residue (*1*). This conserved aromatic residue is linked to the distal histidine by a peptide bond and is situated in helix B, which also contains the distal arginine (Figure 1). The phenyl aromatic ring is located approximately 3.3−3.5 Å above the heme plane (*2*−*4*). Furthermore, the crystal structures of CCP and the W51F mutant show that the phenyl ring occupies a position very similar to that of the six-membered ring of the original tryptophan (*5*). The role of the distal arginine and histidine residues has been investigated by spectroscopic and kinetic studies of various mutants of HRP-C, CCP, and CIP. It has been established that they play a concerted role in the catalytic activity and in stabilizing the heme pocket architecture of the proteins (*6*−*18*). Several studies have also been performed with HRP-C and CCP mutants in an effort to understand the role of the distal W51 in CCP and F41 in HRP-C. In CCP, alteration of W51 has significant effects on the coordination properties and function of the enzyme (*2*, *6*, *19*−*24*). In fact,

† This project was supported by the Italian Consiglio Nazionale delle Ricerche (CNR), the Ministero Universita' e Ricerca Scientifica e Tecnologica (MURST ex 60% and ex 40%, Cofin MURST 97 CFSIB) (to G.S.), and EU Contract BIO4-97-2031 (to G.S. and K.G.W.).

* To whom correspondence should be addressed. E-mail: smulev@chim.unifi.it.

‡ Universita' di Firenze.

§ University of Copenhagen.

|| Novo Nordisk A/S.

⊥ Aalborg University.

[1] Abbreviations: APX, ascorbate peroxidase; ARP, *Arthromyces ramosus* peroxidase; CCP, cytochrome *c* peroxidase; CIP, *Coprinus cinereus* peroxidase expressed in *Aspergillus oryzae*, identical to ARP; HRP-C, horseradish peroxidase isoenzyme C; LIP, lignin peroxidase; MnP, manganese peroxidase; F54Y, Phe54 → Tyr CIP mutant; F54W, Phe54 → Trp CIP mutant; F54G, Phe54 → Gly CIP mutant; F54V, Phe54 → Val CIP mutant; W51F, Trp51 → Phe CCP mutant; W51M, Trp51 → Met CCP mutant; W51T, Trp51 → Thr CCP mutant; W51A, Trp51 → Ala CCP mutant; W51G, Trp51 → Gly CCP mutant; F41V, Phe41 → Val HRP-C mutant; F41W, Phe41 → Trp HRP-C mutant; R51L, Arg51 → Leu CIP mutant; WT, wild-type; RR, resonance Raman; 5-c and 6-c, five-coordinate and six-coordinate heme iron, respectively; HS and LS, high- and low-spin, respectively; 5-c HS*, five-coordinate high-spin heme containing a weak fifth ligand; CT1, long-wavelength (>600 nm) porphyrin-to-metal charge transfer band.

10.1021/bi982811+ CCC: $18.00
Published on Web 05/20/1999

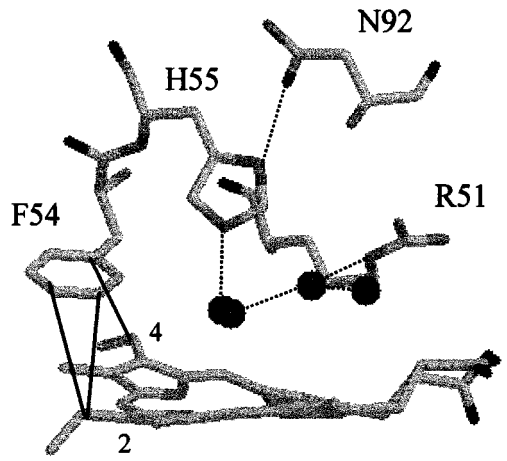

FIGURE 1: Structural diagram of the distal heme pocket of CIP/ARP (*3*). Dashed lines denote inferred hydrogen bonds, on the basis of distance criteria. Solid lines denote the closest distances between carbon atoms of F54 and vinyl 2 and 4 ($C_{\epsilon 2}-C_{ab}$ = 4.09 Å, $C_{\zeta}-C_{ab}$ = 4.13 Å, and $C_{\gamma}-C_{ac}$ = 4.26 Å). Four water molecules are also shown.

this residue forms part of the distal active site near the open coordination position of the heme iron and forms a hydrogen bond with one of the water molecules that is displaced on H_2O_2 binding (*9*, *25*). All the W51 variants examined so far (W51F, W51M, W51T, W51A, and W51G) (*2*, *6*, *19*−*24*, *26*, *27*) showed changes in the state of axial heme coordination. Most of the substitutions resulted in a change of the ferric high-spin heme from a five-coordinate to a six-coordinate form and caused an increased tendency for conversion to a low-spin species at neutral pH. The change of coordination has been explained by the loss of the W51 hydrogen bond to the distal H_2O, which increases the latter's ability to bind the heme iron (*6*, *26*). Moreover, the W51F and W51A have been shown to be more active than the wild-type (wt) enzyme in catalyzing the oxidation of cytochrome *c*, under steady-state conditions, and it has been proposed that the hyperactivity is due to the enhanced reactivity of the oxy−ferryl heme in electron transfer (*19*, *23*). In contrast to the CCP mutants, the replacement of the analogous phenylalanine residue by valine (F41V) in HRP-C caused an 8-fold reduction in the rate of reaction of the enzyme with H_2O_2 (compound I formation) compared with that of HRP-C in transient-state experiments, but a small increase in the rates of oxidation of *p*-aminobenzoic acid by compounds I and II was observed (*28*). The spectroscopic characterization of the F41V HRP-C mutant indicated that the mutation resulted in a change of the ferric high-spin heme from a five-coordinate to a six-coordinate form (*10*). Recently, other F41 HRP-C variants have been reported. Steady-state analysis suggested that the mutation of F41 to alanine (*11*, *29*), leucine, or threonine (*30*, *31*) has only minor effects on HRP-C compound I formation or guaiacol oxidation. More significantly, these mutations greatly increased the ability of HRP-C to catalyze peroxygenase reactions, in which the ferryl oxygen is transferred to the substrate, consistent with the proposal that in the native enzyme the ferryl oxygen is partially shielded from direct interaction with substrates (*30*, *31*).

In this work, we report the characterization by electronic absorption and resonance Raman spectroscopies of the four *C. cinereus* peroxidase (CIP) distal variants F54W (F54W), -Y (F54Y), -V (F54V), and -G (F54G) in both Fe^{3+} and Fe^{2+} states and after complex formation with fluoride and imidazole. The effects of these mutations are compared with those reported for the corresponding HRP-C and CCP mutants.

MATERIALS AND METHODS

CIP mutants were constructed and expressed in *Aspergillus oryzae* (*32*), and the protein samples were purified and prepared as previously described (*33*). Since CIP and the fungal peroxidase *Arthromyces ramosus* peroxidase (ARP) are indistinguishable (*33*), we will refer to this fungal peroxidase by name CIP or CIP/ARP when referring to information taken from the crystal structure of ARP (*3*).

The following buffers were used: 10 mM citric acid/sodium citrate (pH 3.8−5.3), 10 mM sodium phosphate (pH 7.0), 20 mM boric acid/10 mM sodium phosphate (pH 10.0), 10 mM sodium bicarbonate (pH 11.0), and 25 mM borate for the reduced form at pH 10.0. All experiments were performed in 1 mM $CaCl_2$ at a constant ionic strength of 0.1 M adjusted using potassium sulfate. All pH values of >11.0 were obtained by adding degassed NaOH to degassed buffered protein solutions.

Fluoride complexes were obtained in 0.1 M NaF (Merck), citric acid/sodium citrate buffer at pH 5.0 or by adding solid NaF to buffered enzyme solutions when fluoride binding was weak as for the mutant F54Y. Imidazole adducts were obtained by adding solid imidazole (Merck) to the protein solution to a final pH of 10.5.

The Fe^{2+} form was prepared by adding a minimum volume of fresh sodium dithionite solution to a deoxygenated buffered solution.

The sample concentration was about 0.01−0.4 mM for resonance Raman (RR) spectroscopy and about 0.05−0.1 mM for UV−visible absorption measurements.

Absorption spectra were recorded with a Cary 5 spectrophotometer. Absorption spectra were recorded both prior to and after RR measurements, ensuring that no degradation had taken place under the experimental conditions. The RR spectra were obtained by excitation with the 406.7 and 413.1 nm lines of a Kr^+ laser (Coherent, Innova 90/K) and the 457.9 nm line of an Ar^+ laser (Coherent, Innova 90/5). The backscattered light from a slowly rotating NMR tube was collected and focused into a computer-controlled double monochromator (Jobin-Yvon HG 2S) equipped with a cooled photomultiplier (RCA C31034 A) and photon-counting electronics. The RR spectra were calibrated with indene and CCl_4 as standards to an accuracy of 1 cm^{-1} for intense isolated bands.

Polarized spectra were obtained by inserting a polaroid analyzer between the sample and the entrance slit of the spectrometer. The depolarization ratio, ρ, of the bands at 314 and 460 cm^{-1} of CCl_4 was measured to check the reliability of polarization measurements. The values obtained, 0.73 and 0.01, compared favorably with the theoretical values of 0.75 and 0.00, respectively.

All the electronic absorption spectra were collected at room temperature, i.e., at about 23 °C. The RR spectra were collected at approximately 15 °C; the rotating NMR tube was cooled by a gentle flow of N_2 gas passing through liquid N_2 to minimize the local heating of the protein induced by the laser beam.

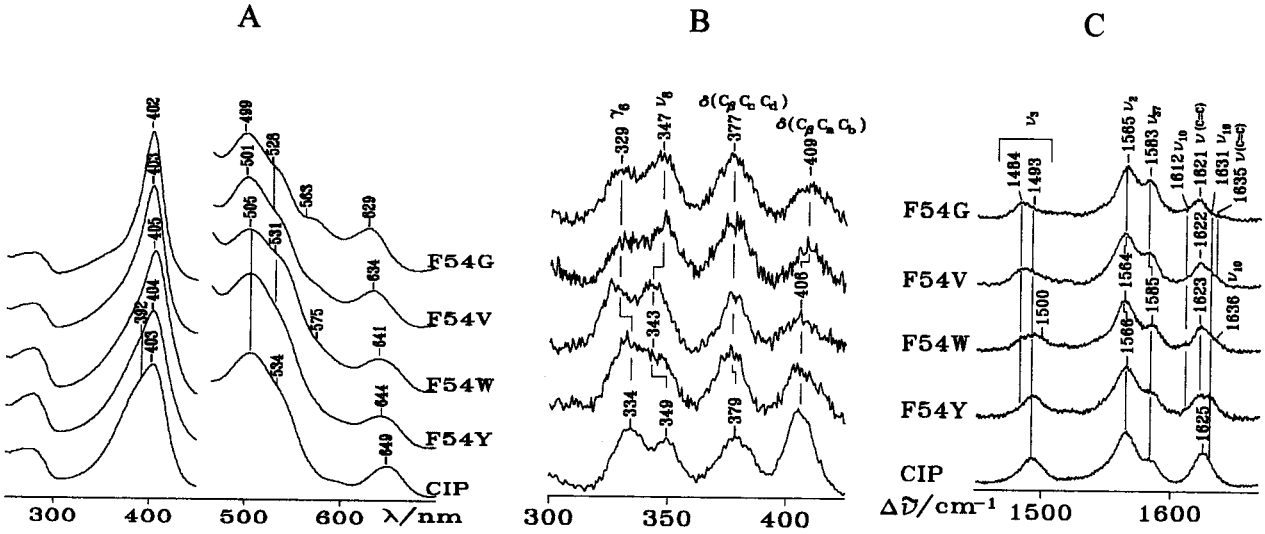

FIGURE 2: (A) Electronic absorption spectra of ferric CIP and the distal mutants F54Y, F54W, F54V, and F54G at pH 7.0. The region between 450 and 700 nm has been expanded 8-fold. (B and C) Resonance Raman spectra of ferric CIP and the distal mutants F54Y, F54W, F54V, and F54G at pH 7.0. Experimental conditions were as follows: 406.7 nm excitation, 15 mW laser power at the sample, and 5 cm^{-1} resolution. (B) For CIP, 5 s/0.5 cm^{-1} collection interval; for F54Y, 25 s/0.5 cm^{-1} collection interval; for F54W, 11 s/0.5 cm^{-1} collection interval; for F54V, 4 s/0.5 cm^{-1} collection interval; and for F54G, 6 s/0.5 cm^{-1} collection interval. (C) For CIP, 8 s/0.5 cm^{-1} collection interval; for F54Y, 13 s/0.5 cm^{-1} collection interval; for F54W, 9 s/0.5 cm^{-1} collection interval; for F54V, 10 s/0.5 cm^{-1} collection interval; and for F54G, 10 s/0.5 cm^{-1} collection interval.

The dissociation constants, K_d, for fluoride−peroxidase complexes were determined by spectrophotometric titrations (*34*).

RESULTS

Figure 2A compares the electronic absorption spectra of WT CIP and its F54Y, F54W, F54V, and F54G mutants obtained at pH 7.0. Significant changes can be seen for some of the mutants. The sharpening and the intensity increase of the Soret band and the concomitant progressive blue shift of the CT1 band in the order F54Y, F54W, F54V, and F54G suggest an increasing proportion of six-coordinate (6-c) high-spin (HS) heme with respect to CIP, which is five-coordinate (5-c) HS (*35*). In fact, a 6-c HS is usually distinguished from a 5-c HS by an increase of the Soret extinction coefficient of about 40%, a concomitant intensity decrease of the shoulder at about 390 nm, that is strongly pronounced in the 5-c HS species, and the blue shift of the CT1 band (*18*). An apparent inconsistency with this interpretation is derived from the overall blue shift of the spectra of both F54V and F54G with respect to the WT protein, since usually a 6-c HS heme exhibits a red-shifted Soret band with respect to the corresponding 5-c HS species (*6*). The reason for the blue shift is discussed below.

Panels B and C of Figure 2 compare the corresponding RR spectra. The high-frequency region (C) indicates that the F54Y mutant does not markedly differ from WT CIP, whereas the other three mutants exhibit an increase in the level of the 6-c HS heme at the expense of the 5-c HS species, as judged by the intensity ratio of the 1484 cm^{-1} versus the 1493 cm^{-1} band assigned to the ν_3 mode. The F54W mutant also shows the presence of a small amount of a 6-c LS heme, as determined by the bands at 1500 cm^{-1} (ν_3) and 1636 cm^{-1} assigned to the ν_{10} mode since it is depolarized in the spectra recorded in polarized light (Figure 3, top). Moreover, the spectra in polarized light show that the ν(C═C) stretching modes of the vinyl groups change their frequency upon mutation. In particular, the two ν(C═C) bands found to overlap at about 1625 cm^{-1} in CIP (*35*) are at 1623 cm^{-1} in both F54Y (not shown) and F54W and give rise to two separated bands at 1621−1622 and 1635 cm^{-1} in the F54V and F54G mutants. The band at the higher frequency is very weak and, in the F54V mutant, almost hidden by the band at 1631 cm^{-1} due to the ν_{10} mode of the 5-c HS species (Figure 3, top). An indirect confirmation of the upshift of the vinyl stretch frequency is derived from the frequency of the ν_2 mode. In fact, it is known that the ν_2 mode is coupled to the vinyl ν(C═C) mode in protohemes, and saturation of the vinyl groups raises the ν_2 frequencies by about 10 cm^{-1} (*36*). In 6-c HS protoporphyrin IX model compounds, exhibiting the ν(C═C) stretching modes at 1621 cm^{-1}, the ν_2 was found at 1560 cm^{-1} (*36*). The frequency of the ν_2 mode in both F54V and F54G is at 1565 cm^{-1}, 5 cm^{-1} higher than those for the model compounds. A vinyl stretch frequency of 1635 cm^{-1} is extremely high, indicating a fairly low degree of conjugation between the vinyl double bond and the porphyrin macrocycle. A lower degree of conjugation of the vinyl mode can explain the overall blue shift of the UV−vis spectra observed for the F54V and F54G mutants, as previously found for ascorbate peroxidase (APX) as compared to CCP (*37*).

In the low-frequency region (Figure 2B), the broad band at 406 cm^{-1} of CIP, assigned to the $\delta(C_\beta C_a C_b)$ bending modes of the vinyl substituents, shifts up by 3 cm^{-1} in the F54V and F54G mutants in accord with the frequency changes observed in the high-frequency region and in agreement with the previous observation for CCP at alkaline pH (*38*). The other major changes observed in the low-frequency region can be predominantly ascribed to the increase in the level of the 6-c HS at the expense of the 5-c HS heme. In particular, the band at 334 cm^{-1} of CIP shifts down and decreases in intensity on passing from F54Y to F54G. This band is assigned to the out-of-plane vibration, γ_6, by analogy with CCP. It has been found to be intense in

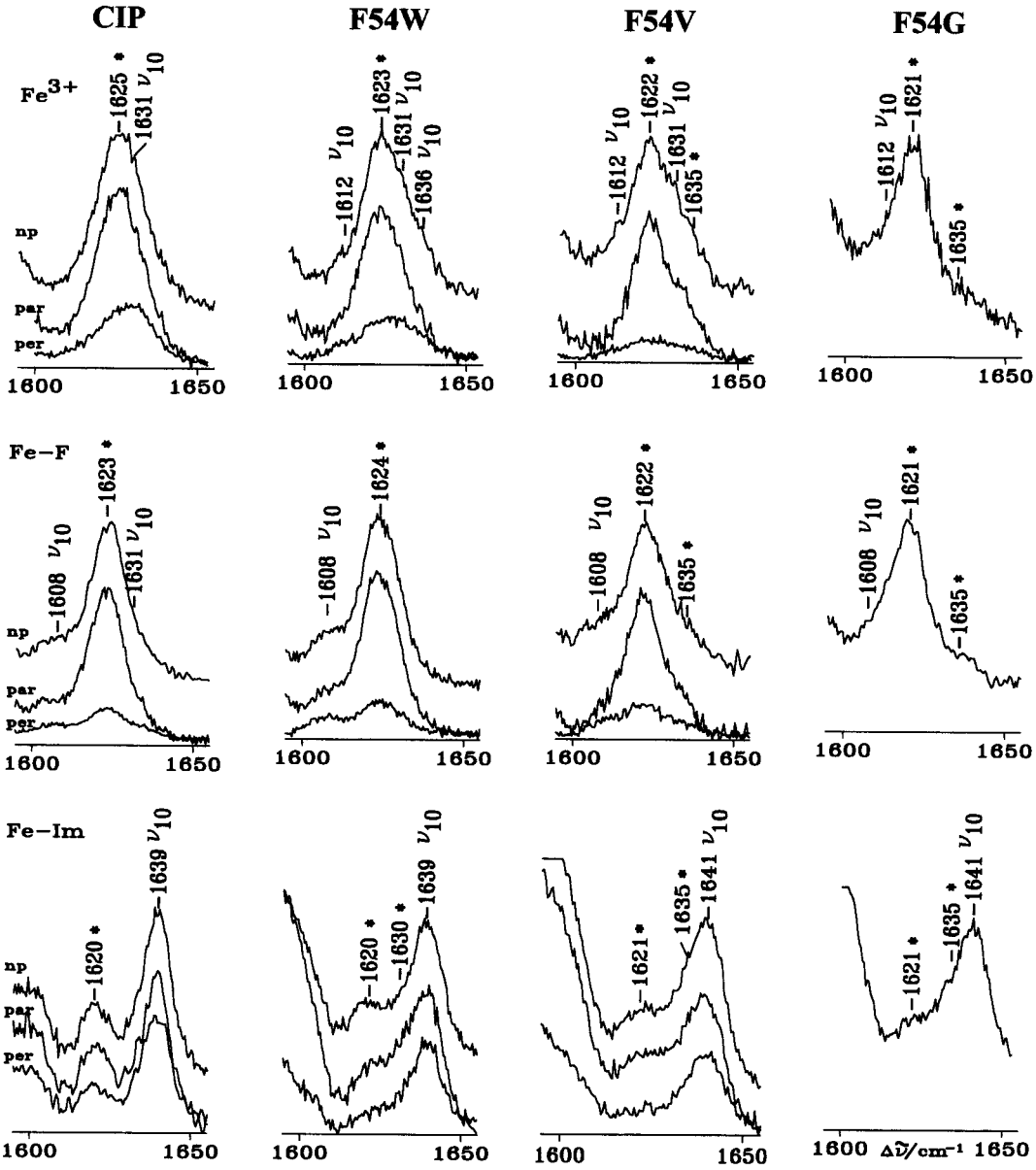

FIGURE 3: Resonance Raman spectra of the ferric form (top), the fluoride complex (middle), and the imidazole complex (bottom) of CIP and the F54W, F54V, and F54G mutants in the region of 1600−1650 cm^{-1}. Experimental conditions were as follows: 5 cm^{-1} resolution, 406.7 nm excitation, 25 mW laser power at the sample for the ferric and the fluoride complexes, and 30 mW at the sample for the imidazole complexes. (Top) For CIP, nonpolarized, np, 15 s/0.5 cm^{-1}, parallel polarization, par, 12 s/0.5 cm^{-1}, perpendicular polarization, per, 24 s/0.5 cm^{-1}; for F54W, np, 42 s/0.5 cm^{-1}, par, 33 s/0.5 cm^{-1}, per, 60 s/0.5 cm^{-1}; for F54V, np, 22 s/0.5 cm^{-1}, par, 23 s/0.5 cm^{-1}, per, 36 s/0.5 cm^{-1}; for F54G, np, 15 s/0.5 cm^{-1}. (Middle) For CIP, np, 12 s/0.5 cm^{-1}, par, 8 s/0.5 cm^{-1}, per, 24 s/0.5 cm^{-1}; for F54W, np, 15 s/0.5 cm^{-1}, par, 15 s/0.5 cm^{-1}, per, 18 s/0.5 cm^{-1}; for F54V, np, 34 s/0.5 cm^{-1}, par, 18 s/0.5 cm^{-1}, per, 34 s/0.5 cm^{-1}; for F54G, np, 30 s/0.5 cm^{-1}. (Bottom) For CIP, np, 48 s/0.5 cm^{-1}, par, 30 s/0.5 cm^{-1}, per, 48 s/0.5 cm^{-1}; for F54W, np, 68 s/0.5 cm^{-1}, par, 48 s/0.5 cm^{-1}, per, 48 s/0.5 cm^{-1}; for F54V, np, 78 s/0.5 cm^{-1}, par, 48 s/0.5 cm^{-1}, per, 36 s/0.5 cm^{-1}; for F54G, np, 24 s/0.5 cm^{-1}; the asterisk denotes the bands assigned to the ν(C═C) vinyl stretches.

the 5-c HS heme state, a shoulder in the 6-c HS heme, and absent in the 6-c low-spin (LS) heme. Furthermore, its frequency also varies considerably with the coordination and spin state of the heme Fe and with its oxidation state (*38*).

Titration of the mutated proteins shows that the coordination and spin state depend on pH. The F54G and F54V mutants do not appreciably change between pH 5.0 and 7.0 (data not shown), being mainly 6-c HS, whereas at pH ≥11, the proteins become 6-c LS heme with a concomitant loss of heme, as judged by the broadening of the Soret band with the appearance of an intense shoulder at about 380 nm. In contrast, the F54W and F54Y proteins are extremely sensitive to pH.

Figure 4 (left) shows the electronic absorption spectra of F54Y between pH 4 and 11.0. Two distinctive transitions are seen, at pH <7 and at pH >10. The first transition is associated with a red shift of the Soret band, its concomitant increase in intensity, and the disappearance of the shoulder at about 380 nm, and the blue shift of the CT1 band by 6 nm on passing from pH 4.0 to 7.0. These changes are consistent with the formation of a 6-c HS heme at the expense of a 5-c HS species on going from acidic to neutral pH. The RR spectra recorded at acidic pH confirmed this interpretation (data not shown), but the sample appeared to be extremely unstable, giving rise to irreversible changes upon laser illumination. At pH 11.0, the protein shows the

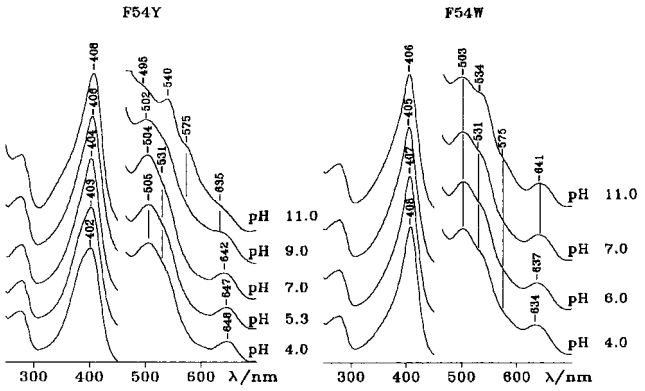

FIGURE 4: Electronic absorption spectra of ferric F54Y (left) and F54W (right) obtained at various pH values. The region between 450 and 700 nm has been expanded 8-fold.

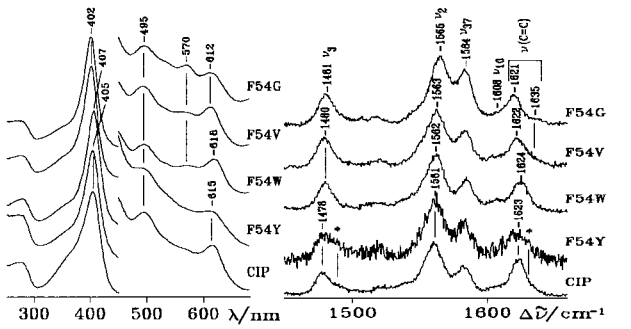

FIGURE 5: Electronic absorption (left) and resonance Raman (right) spectra of the fluoride complexes of ferric CIP and the distal mutants F54Y, F54W, F54V, and F54G at pH 5.0. (Left) The region between 450 and 700 nm has been expanded 8-fold. (Right) The experimental conditions were as follows: 406.7 nm excitation, 15 mW laser power at the sample, and 5 cm^{-1} resolution. For CIP, 3 s/0.5 cm^{-1} collection interval; for F54Y, 3 s/0.5 cm^{-1} collection interval; for F54W, 5 s/0.5 cm^{-1} collection interval; for F54V, 9 s/0.5 cm^{-1} collection interval; and for F54G, 21 s/0.5 cm^{-1} collection interval. The asterisk denotes the band of the 5-c HS unligated proteins at 1493 cm^{-1} (ν_3) and 1631 cm^{-1} (ν_{10}).

presence of a 6-c LS heme similar to that observed for the WT protein at pH 12.1 (*35*) and, therefore, is interpreted as due to a hydroxyl ligand bound to the heme iron.

Figure 4 (right) shows the electronic absorption spectra of F54W obtained between pH 4.0 and 11.0. On the pH being raised from 4.0 to 7.0, the blue shift of the Soret band and the red shift of the CT1 band are consistent with the decrease in the level of a 6-c HS heme and the formation of a 5-c HS species. The transition appears to be completed at pH 5.0 since its electronic absorption spectrum (data not shown) is identical to the one recorded at pH 4.0. At pH 11.0, a low-spin heme is present, though some 5-c and 6-c HS forms appear to remain, rendering an estimate of the amount of the alkaline form present difficult. Nevertheless, it appears that, as for F54Y, the pK_a of the alkaline transition is lower than for the wild type, since at pH 11.0 no low-spin heme was observed in CIP (*33*).

To understand the role of F54 in ligand binding, the ability of the mutants to react with fluoride (pH 5.0) or imidazole (pH 10.5) was investigated. Figure 5 (left) compares the electronic absorption spectra of the fluoride complexes obtained at pH 5.0. Heme proteins bind fluoride giving rise to 6-c HS hemes. As previously reported, WT CIP does not bind the anion completely (*39*, *40*), giving rise to a mixture of 5- and 6-c HS hemes, with the latter being predominant. F54Y binds fluoride even more poorly than the WT protein, whereas F54W, F54V, and F54G mutants bind the ligand completely, as judged by the electronic absorption and RR spectra (see below). In previous work, it has been found that the distal aromatic residue in position 54 is particularly important for stabilizing the fluoride anion (*37*, *40*). In particular in CCP and APX, where a tryptophan residue is conserved in the position corresponding to F54 of CIP (*41*), the fluoride is stabilized by a hydrogen bond from the indole nitrogen (*37*, *40*, *42*). Moreover, it is seen that replacement of the distal F54 with W in CIP not only increases the fluoride affinity but also causes a red shift of the CT1 band maximum, making it very similar to that of CCP, suggesting that the mutated residue is hydrogen bonded to the ligand (*40*). These previous results are confirmed in this work as the F54W mutation increases the stability of the fluoride complex by about 4500-fold (at pH 4.85, $K_d = 0.4 \pm 1.0$ μM for the mutant and 18 ± 6 mM for CIP). Interestingly, the dissociation constant for the fluoride complex of the mutant becomes similar to that found for WT CCP (*43*, *44*). The 6-c F54V and F54G mutants also appear to bind fluoride better than the 5-c CIP, despite the lack of hydrogen bond stabilization by the valine and glycine side chains, as indicated by the sharp Soret band and the appearance of the band at 570 nm, associated with the fluoride complex. Both the Soret and the CT1 bands are 4 and 3 nm blue-shifted with respect to those of CIP due to the vinyl reorientation (see below).

The corresponding RR spectra (Figure 5, right) confirm the conclusions drawn from the UV−vis spectra. F54Y binds fluoride very poorly, whereas for the F54W, F54V, and F54G mutants, no residual 5-c HS is detected upon fluoride binding. In addition, the formation of a 6-c HS heme and, therefore, the shift of the ν_{10} from 1631 (5-c HS) to 1608 cm^{-1} (6-c HS) allow us to measure the frequency of the vinyl stretching mode in a more precise way than for the free proteins. Figure 3 (middle) shows the 1600−1660 cm^{-1} region recorded in polarized light. As previously found for the noncomplexed forms, the F54V and F54G mutants are characterized by two ν(C═C) stretching modes at 1622 cm^{-1} (F54V) (1621 cm^{-1} for the F54G mutant) and at 1635 cm^{-1}. Accordingly, the ν_2 mode shifts from 1561 cm^{-1} in CIP to 1563 cm^{-1} in F54V and 1565 cm^{-1} in F54G (Figure 5, right). Therefore, the blue shift of the Soret and CT1 bands can be ascribed to a vinyl double bond, which is less conjugated with the porphyrin macrocycle.

The RR frequency of the ν(Fe−F) stretching mode in the low-frequency region would provide direct evidence for hydrogen bonding of the fluoride ligand to distal residues in CIP and its F54W mutant. The fluoride complexes of metmyoglobin and methemoglobin show ν(Fe−F) stretches at about 460−420 and 470−440 cm^{-1}, respectively, upon excitation in both the CT1 and 441.6 nm regions (*45*−*49*). Moreover, the higher-frequency band is pH sensitive, as it shifts down by about 60 cm^{-1} upon acidification. This result was interpreted as being due to protonation of the distal His and formation of a hydrogen bond to the fluoride ligand (*49*). For HRP-C, the ν(Fe−F) stretch is observed at 385 cm^{-1} upon excitation in the CT1 band. The fact that the frequency of HRP-C is lower than that of the globins is in agreement with the presence of stronger hydrogen bonding between the fluoride and distal residues (*50*). Therefore, we attempted

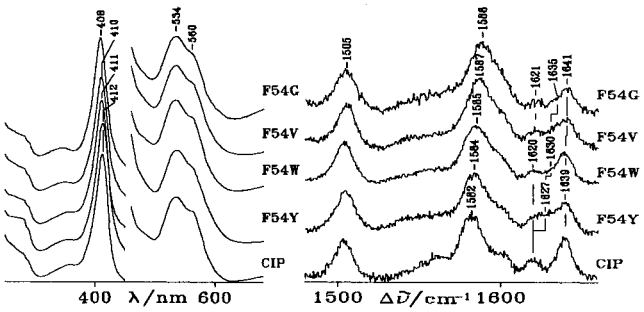

FIGURE 6: Electronic absorption (left) and resonance Raman (right) spectra of the imidazole complexes of ferric CIP and the distal mutants F54Y, F54W, F54V, and F54G at pH 10.5. (Left) The region between 450 and 700 nm has been expanded 8-fold. (Right) The experimental conditions were as follows: 406.7 nm excitation, 20 mW laser power at the sample, and 5 cm^{-1} resolution. For CIP, 18 s/0.5 cm^{-1} collection interval; for F54Y, 21 s/0.5 cm^{-1} collection interval; for F54W, 30 s/0.5 cm^{-1} collection interval; for F54V, 21 s/0.5 cm^{-1} collection interval; and for F54G, 29 s/0.5 cm^{-1} collection interval.

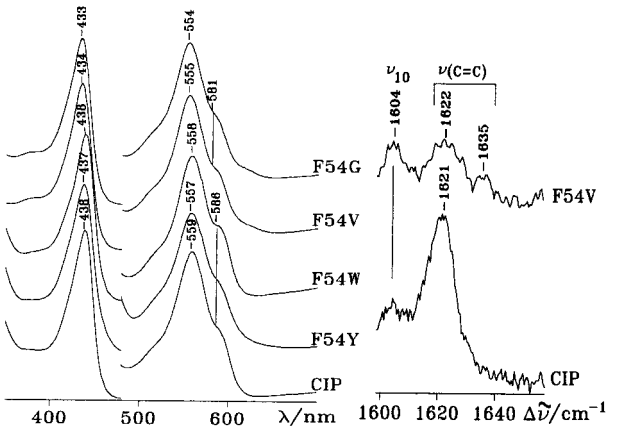

FIGURE 7: (Left) Electronic absorption spectra of ferrous CIP and distal mutants F54Y, F54W, F54V, and F54G at pH 6.0. The region between 450 and 700 nm has been expanded 8-fold. (Right) Resonance Raman spectra of Fe^{2+} CIP and the distal mutant F54V at pH 6.0. Experimental conditions were as follows: 457.9 nm excitation, 15 mW laser power at the sample, and 5 cm^{-1} resolution. For CIP, 8 s/0.5 cm^{-1} collection interval; and for F54V, 34 s/0.5 cm^{-1} collection interval.

to find the ν(Fe−F) stretching mode of HRP-C, CCP, and CIP fluoride complexes using Soret excitation (from 406.7 to 457.9 nm), which is available to us. However, no band exhibited sensitivity to changes of the exciting wavelength, and therefore, no band could be assigned to the fluoride ligand. The ν(Fe−F) stretch in peroxidases, therefore, appears to be very weak and possibly overlapped with the propionyl bending modes (observed in the fluoride complexes around 380 cm^{-1}), if resonance enhanced with Soret band excitations. Interestingly, the OH^- ligand, isoelectronic with the F^-, showed a Soret enhanced RR ν(Fe−OH) stretch that was also much weaker in peroxidases (*15*, *51*, *52*) than in globins (*52*). The different intensity behavior observed for the ν(Fe−F) and ν(Fe−OH) stretches might be due to the presence of stronger hydrogen bonds between the ligand and the distal residues in peroxidases than in globins.

Figure 6 (left) compares the electronic absorption spectra of the imidazole complexes obtained for CIP and the four mutants at pH 10.5. All the spectra are characteristic of a 6-c LS heme with two nitrogen atoms bound to the heme iron, as suggested by the wavelength maxima in the visible region at 534 and 560 nm (*7*). The spectra of F54W and F54V exhibit a Soret band, which is 1 and 2 nm, blue-shifted with respect to CIP; the blue shift is even greater for the F54G mutant (4 nm). Figure 6 (right) compares the corresponding RR spectra in the high-frequency region. All the spectra exhibit core-size marker bands typical of a 6-c LS heme. Differences are observed in the vinyl stretching modes as observed in Figure 3 (bottom), which shows the RR spectra in the 1600−1650 cm^{-1} region recorded in polarized light. The CIP complex is characterized by the polarized band at 1620 cm^{-1}, due to the vinyl stretches, which is well separated from the depolarized band at 1639 cm^{-1} due to the ν_{10} mode. On the contrary, the spectra of all the mutants do not exhibit two distinct bands in this region, and on the basis of the spectra recorded in polarized light, two vinyl stretches together with the ν_{10} mode can be assigned. One is at about the same frequency as CIP, and the other is upshifted by about 7, 10, 15, and 15 cm^{-1} in F54Y, F54W, F54V, and F54G, respectively. Concomitantly, as previously observed for both the ferric and fluoride complexes, with the increase of the frequency of one vinyl stretch, the ν_2 mode frequency shifts up by 2, 3, 5, and 6 cm^{-1}, respectively (Figure 6, right), indicating a lower degree of vibrational coupling with the ν(C═C) vinyl stretches.

Figure 7 (left) compares the electronic absorption spectra of the reduced form of the mutants and the WT protein recorded at pH 6.0. All the spectra are characteristic of 5-c HS hemes, but whereas CIP, F54Y, and F54W differ only slightly in their wavelength maxima, the spectra of F54V and F54G are blue-shifted by about 4 nm with respect to the WT protein. The RR spectra (data not shown) confirm that the proteins are all pure 5-c HS. The blue shift of the electronic spectra of F54V (as probably that of F54G) is due to the reduced level of conjugation of one vinyl mode as shown in Figure 7 (right), where the RR spectra in the 1600−1660 cm^{-1} region of Fe^{2+} CIP and Fe^{2+} F54V are reported. It can be seen that whereas in the WT protein the two ν(C═C) stretching modes overlap at 1621 cm^{-1}, the F54V mutant is characterized by two distinct stretches at 1622 and 1635 cm^{-1}, as found for the ferric heme. The spectra of reduced F54W and F54Y are very similar to that of WT CIP (data not shown); the spectrum of F54G has not been checked because of the lack of a sample.

At pH 10.0, only the F54V mutant (in the Fe^{2+} form) remains 5-c HS, as the WT protein (*35*). Both F54Y and F54W are a mixture of 5-c HS and 6-c LS hemes. The F54G has not been analyzed because of the lack of a sample. The low-spin heme might derive from a change in the distal cavity which induces the distal histidine to bind directly to the heme iron, as previously observed for both Fe^{3+} and Fe^{2+} CCP at alkaline pH (*7*). As a consequence of the presence of a low-spin heme, we undertook the study of the RR low-frequency region only for those mutants whose spectra are characteristic of a 5-c HS heme. In fact, in the low-frequency region, the main information is given by the frequency of the ν(Fe−Im) stretching mode, detected only in the 5-c Fe^{2+} heme proteins, which in peroxidases is fairly high and pH-dependent. Both of these features have been attributed to the presence of a hydrogen bond between N_δ of the imidazole ligand and the oxygen atom of an aspartic residue (*53*). In CIP, the Fe^{2+}-His RR band has two components with

Table 1: Absorption Maxima (nm) of Soret and CT1 Bands and RR Frequencies (cm^{-1}) of the ν_2 and ν(C=C) Vinyl Stretching Modes Observed for the Various Forms of CIP and Phe54 Mutants

protein	spin state[a]	Soret (nm)	CT1 (nm)	ν_2 (cm^{-1})	ν(C=C) (cm^{-1})[b]
		Fe^{3+} at pH 7.0			
CIP[c]	5-c HS	403	649	1566	1625
Phe54Tyr	5-c HS, 6-c HS	404	644	1566	1623
Phe54Trp	5-c HS, 6-c HS, 6-c LS	405	641	1564	1623
Phe54Val	5-c HS, 6-c HS	403	634	1565	1622, 1635
Phe54Gly	5-c HS, 6-c HS	402	629	1565	1621, 1635
		Fe^{3+}−F at pH 5.0			
CIP[d]	5-c HS, 6-c HS	405	615	1561	1623
Phe54Tyr	5-c HS, 6-c HS	405	615	1561	1623
Phe54Trp	6-c HS	407	618	1562	1624
Phe54Val	6-c HS	402	612	1563	1622, 1635
Phe54Gly	6-c HS	402	612	1565	1621, 1635
		Fe^{3+}−Im at pH 10.5			
CIP	6-c LS	412		1582	1620
Phe54Tyr	6-c LS	412		1584	1620, 1627
Phe54Trp	6-c LS	411		1585	1620, 1630
Phe54Val	6-c LS	410		1587	1621, 1635
Phe54Gly	6-c LS	408		1588	1621, 1635
		Fe^{2+} at pH 6.0			
CIP[c]	5-c HS	438		1559	1621
Phe54Tyr	5-c HS	437		1561	1622
Phe54Trp	5-c HS	438		1559	1621
Phe54Val	5-c Hs	434			1622, 1635
Phe54Gly	5-c Hs	433			

[a] The most abundant species is underlined. [b] The most intense band is underlined. [c] From ref *35*. [d] From ref *40*.

frequencies at 230 and 211 cm^{-1}. The 230 cm^{-1} component is more intense at neutral pH, whereas at alkaline pH, the intensity of the band at 211 cm^{-1} increases at the expense of the band at 230 cm^{-1}. This shift has been interpreted as being due to changes associated with protonation of the proximal His residue. The ν(Fe−Im) stretching mode at 230 cm^{-1} suggests the presence of a hydrogen-bonded imidazole, whereas the 211 cm^{-1} band suggests the presence of a fairly weak hydrogen bond interaction between $N_\delta H$ of the proximal H183 and the oxygen atom of the D245 side chain (*35*). Since no appreciable changes in the frequencies of the ν(Fe−Im) stretching modes have been observed in the mutants (data not shown), it appears that the distal mutation does not affect the proximal hydrogen bond strength, in agreement with the previous findings for the F41V mutant of HRP-C (*10*) and the W51F mutant of CCP (*6*).

Table 1 summarizes the wavelengths of the Soret and CT1 bands and the frequencies of the ν_2 and ν(C=C) stretching modes together with their coordination and spin states, observed for the various forms of CIP and its F54 mutants.

DISCUSSION

This analysis indicates that substitution of the distal phenylalanine in CIP causes alterations in the distal cavity, which were also partly observed for the corresponding mutations in CCP and HRP-C. The distal F54 in CIP plays an important role in maintaining the architecture of the distal cavity. Despite the fact that the aromatic phenyl group is not directly involved in the hydrogen bonding network with the water molecules, its substitution with either a hydrogen bond acceptor/donor (tyrosine), a hydrogen bond donor (tryptophan), or small aliphatic residues (glycine and valine) gives rise to an aquo 6-c HS species. The results suggest also that the heme pocket undergoes a readjustment depending on the size and hydrogen bonding ability of the residue inserted at position 54 of CIP. When the aromatic ring of the phenyl group is replaced by valine and glycine, both the vinyl groups of the heme chromophore change their ν(C=C) stretching mode frequency, indicating a marked change in their orientations in all the forms under investigation. Recently, on the basis of the RR spectra and local density functional calculations on mono- and divinylhemins, it has been proposed that when the protein matrix exerts no constraints on the vinyl groups, two distinct ν(C=C) stretching modes should be observed in their RR spectrum (*54*). Moreover, it has been found that the protein matrix plays a role in directing the orientation of the vinyl groups of the heme chromophore in peroxidases. In particular, in APX and all class III peroxidases, both vinyl groups, which are largely unconstrained by the protein matrix, assume the preferred conformation characterized by two distinct RR ν(C=C) stretching modes, at about 1620 and 1630 cm^{-1}, with only one vinyl group (1620 cm^{-1}) well-conjugated with the double bonds of the heme group (*37*). CIP at pH 7.0 exhibits two vinyl ν(C=C) stretching modes overlapping at 1625 cm^{-1} (*35*), in contrast to the two independent bands at 1621 and 1635 cm^{-1} observed in the F54V and F54G mutants. This suggests that both the vinyl groups are restrained by the distal phenylalanine in the WT protein, and therefore, the replacement of the phenyl ring with the smaller aliphatic side chains of valine and glycine appears to release the constraints on the vinyl substituents. Analysis of the crystal structure of CIP/ARP (*3*, *55*) confirms this hypothesis. As shown in Figure 1, the $C_{\epsilon 2}$, C_ζ, and $C_{\delta 2}$ atoms of the aromatic group are about 4.1−4.2 Å from the C_a atom of the vinyl groups. Interestingly, CIP appears to be different from HRP-C in this respect as the corresponding mutation of HRP-C (F41V) did not exhibit important changes in the frequency of the double bonds of the vinyl groups compared with the WT protein (*10*). A vinyl mode occurs at high frequencies for both the mutant and the wild-type protein.

A change in size of the distal pocket upon mutation is also clearly indicated by ligand binding. Imidazole binding to the F54W and F54Y mutants causes a reorientation of the vinyl double bonds, as judged by the appearance of two RR ν(C=C) stretching frequencies in the imidazole complex. This might indicate that the sterically encumbered imidazole is able to push away the aromatic rings of both Y and W. Since the imidazole binds completely in WT CIP with no appreciable changes in the vinyl stretch frequencies, it appears that the indole and phenol rings of the inserted W and Y residues are closer to the heme than the phenyl ring in the WT protein but must move away from the proximity of the heme iron to allow the imidazole to bind.

Furthermore, mutation alters the fluoride binding capability. Fluoride binds more poorly to the F54Y mutant than to WT CIP. It has been widely accepted that distal histidine is the proton acceptor for the transient binding of peroxide during compound I formation (*56*) as well as for fluoride binding via HF in peroxidases (*43*, *57*). The loss of this acceptor by protonation decreases the bimolecular rate of HF binding and hence the affinity. Moreover, it has been proposed that the distal histidine contributes to the stability of the fluoride complex in peroxidase by hydrogen bonding,

through a water molecule to the anion (*56*). A tyrosine residue can act both as a hydrogen bond acceptor and donor to water molecules in the distal cavity and, thereby, interfere with optimal hydrogen bonding stabilization of the fluoride complex. The F54W mutant binds fluoride much better than CIP. This observation can be simply explained by recalling that the nitrogen atom of the indole ring acts as a hydrogen bond donor with the bound fluoride, stabilizing the ligand. Therefore, the mutation not only increases the affinity for the fluoride by 4500-fold but also causes a red shift of the CT1 band of 3 nm with respect to the parent enzyme due to the bound fluoride being accepting a hydrogen bond from the distal arginine, tryptophan, and a water molecule, exactly as in WT CCP (*44*). Moreover, the lower affinity for the fluoride ligand of WT CIP as compared to that of HRP-C (which also contains a distal phenylalanine) has been suggested to be a consequence of the different position of the distal arginine (R51) in the cavity (*40*). In WT ARP/CIP, the guanidinium group of R51 is 1.7 Å further away from the heme iron (*3*) than in HRP-C (*4*). Since the distal arginine has been found to be a determinant in controlling the ligand binding via a strong hydrogen bond between the positively charged guanidinium group and the anion in peroxidases (*17*, *40*), the longer distance between the arginine and the Fe atom could be responsible for a weaker interaction upon fluoride binding. The fact that both F54V and F54G mutants bind fluoride better than WT CIP might be ascribed to a small displacement of the distal helix B toward the heme, as a consequence of the replacement of the phenyl ring with small aliphatic side chains.

The substitution of F54 by W or Y in CIP gives rise to opposing effects on the coordination state of the heme iron on going from neutral to acidic pH. Hence, at pH 4, the F54Y variant is almost pure 5-c HS heme, whereas acidification drives the F54W to a complete 6-c HS species. For both mutants, the transition occurs at pH <6. An acid transition at pH 5.0 has been observed in WT CIP for cyanide binding (*58*) and compound I formation (*59*). Since the distal His (H55) is generally expected to have a very low pK_a due to the effect of the nearby positively charged distal R51 and the hydrogen bond between the $N_{\delta 1}$ of H55 and the $O_{\delta 1}$ of an asparagine (N92, Figure 1), common to peroxidases, the transition has been associated with protonation of the proximal His (H183) (*14*). In fact, at pH 3.8 a new five-coordinate high-spin form (5-c HS*) characterized by a blue-shifted Soret maximum (394 nm) was identified for WT CIP and assigned to a weakened or broken proximal ligand bond to the heme iron, resulting from protonation of the proximal H183 (*33*). More recently, the R51L mutant of CIP at pH 7.0 exhibited a blue-shifted Soret band very similar to that observed for CIP at acidic pH, and the RR spectrum of the Fe^{2+} form exhibited the presence of a predominant species with a longer Fe−N_ϵ bond with respect to CIP (*17*). In these cases, we do not have any evidence that acidification causes a weakening of the proximal Fe−His bond. In fact, a marked blue shift of the Soret band can be expected when the proximal histidine is replaced by a weaker ligand (*60*−*62*), but the electronic absorption spectra of F54Y and F54W at pH 4.0 are not blue-shifted as in WT CIP at acidic pH. The wavelength of the Soret band is similar to those of other heme proteins, either in their five- or six-coordinate state, containing an imidazole or imidazolate as a fifth ligand.

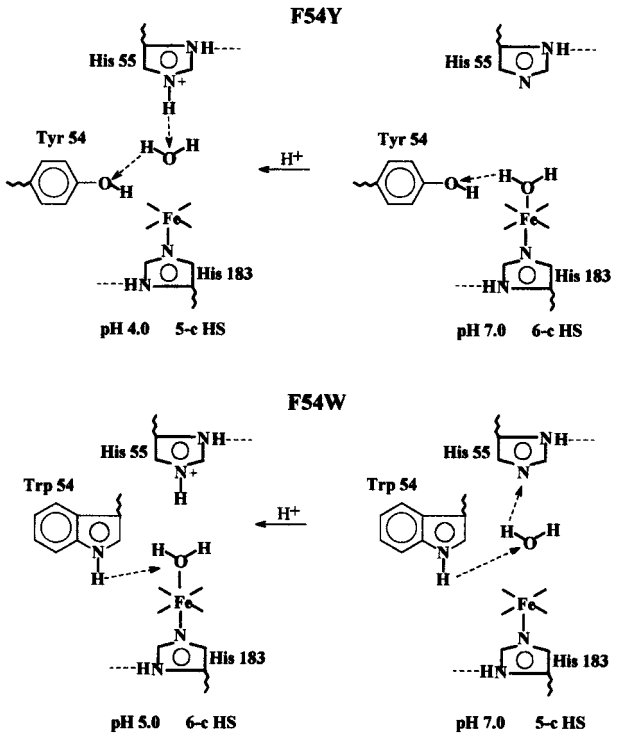

FIGURE 8: Schematic representation of the acidic−neutral ligation equilibrium for F54Y (top) and F54W (bottom) inferred from the spectroscopic data. At neutral pH, the 5-c and 6-c HS forms are present in both mutants. The 5-c HS form is the most abundant in the F54Y mutant, and the 6-c HS form is the most abundant in the F54W mutant (see Table 1).

Moreover, their Fe^{2+} RR spectra do not show appreciable changes in the ν(Fe−Im) stretching mode frequency to indicate that the Fe−Im bond is weaker than in the wild-type protein. On the other hand, the acid transition observed for both the F54Y and F54W variant at pH <6 cannot be explained by protonation of the inserted new residue. In fact, the hydroxyl group of the tyrosine side chain ionizes at alkaline pH near 10.5, and the nitrogen atom of the indole ring of tryptophan can act only as a hydrogen bond donor over the entire pH range (*63*). However, the increased polarity of the distal pocket will assist in charge delocalization. Therefore, we tentatively assign the acid transition observed in the two mutants to the protonation of the distal H55 of CIP. On this basis, the 5-c HS heme observed for the F54Y mutant at pH 4.0 might be derived from the concomitant donation of a hydrogen bond from the distal H55 to the water molecule and from the water molecule to the Y54 (Figure 8, top). In the case of W54, the nitrogen atom can act only as a hydrogen bond donor, therefore, competing with the proton donation of the distal H55 and resulting in a 6-c HS form at acidic pH and a 5-c HS form at neutral pH (Figure 8, bottom).

ACKNOWLEDGMENT

We thank Ms. Yvonne Berger Larsen for purifying the peroxidases, Dr. Christine Bruun Schiødt for measuring the K_d of the fluoride complexes of CIP and the F54W mutant, and Professor Mario P. Marzocchi for many helpful discussions.

REFERENCES

1. Jespersen, H. M., Kjærsgård, V. H., Welinder, K. G., and Østergaard, L. (1997) *Biochem. J. 326*, 305−310.

2. Wang, J., Mauro, J. M., Edwards, S. L., Oatley, S. J., Fishel, L. A., Ashford, V. A., Xuong, N., and Kraut, J. (1990) *Biochemistry 29*, 7160−7173.
3. Kunishima, N., Amada, F., Fukuyama, K., Kawamoto, M., Matsunaga, T., and Matsubara, H. (1996) *FEBS Lett. 378*, 291−294.
4. Gajhede, M., Schuller, D. J., Henriksen, A., Smith, A. T., and Poulos, T. L. (1997) *Nat. Struct. Biol. 4*, 1032−1038.
5. Mondal, M. S., Goodin, D. B., and Armstrong, F. A. (1998) *J. Am. Chem. Soc. 120*, 6270−6276.
6. Smulevich, G., Mauro, J. M., Fishel, L. A., English, A. M., Kraut, J., and Spiro, T. G. (1988) *Biochemistry 27*, 5486−5492.
7. Smulevich, G., Miller, M. A., Kraut, J., and Spiro, T. G. (1991) *Biochemistry 30*, 9546−9558.
8. Vitello, L. B., Erman, J. E., Miller, M. A., Wang, J., and Kraut, J. (1993) *Biochemistry 32*, 9807−9818.
9. Miller, M. A., Shaw, A., and Kraut, J. (1994) *Nat. Struct. Biol. 1*, 524−531.
10. Smulevich, G., Paoli, M., Burke, J. F., Sanders, S. A., Thorneley, R. N. F., and Smith, A. T. (1994) *Biochemistry 33*, 7398−7407.
11. Newmyer, S. L., and Ortiz de Montellano, P. R. (1995) *J. Biol. Chem. 270*, 19430−19438.
12. Rodriguez-Lopez, J. N., Smith, A. T., and Thorneley, R. N. F. (1996) *J. Biol. Inorg. Chem. 1*, 136−142.
13. Rodriguez-Lopez, J. N., Smith, A. T., and Thorneley, R. N. F. (1996) *J. Biol. Chem. 271*, 4023−4030.
14. Abelskov, A. K., Smith, A. T., Rasmussen, C. B., Dunford, H. B., and Welinder, K. G. (1997) *Biochemistry 36*, 9453−9463.
15. Howes, B. D., Rodriguez-Lopez, J. N., Smith, A. T., and Smulevich, G. (1997) *Biochemistry 36*, 1532−1543.
16. Tanaka, M., Ishimori, K., Mukai, M., Kitagawa, T., and Morishima, I. (1997) *Biochemistry 36*, 9889−9898.
17. Neri, F., Indiani, C., Welinder, K. G., and Smulevich, G. (1998) *Eur. J. Biochem. 251*, 830−838.
18. Smulevich, G. (1998) *Biospectroscopy 4*, S3−S17.
19. Goodin, D. B., Mauk, A. G., and Smith, M. (1987) *J. Biol. Chem. 262*, 7719−7724.
20. Fishel, L. A., Villafranca, J. E., Mauro, J. M., and Kraut, J. (1987) *Biochemistry 26*, 351−360.
21. Roe, J. A., and Goodin, D. B. (1993) *J. Biol. Chem. 268*, 20037−20045.
22. Turano, P., Ferrer, J. C., Cheesman, M. R., Thomson, A. J., Banci, L., Bertini, I., and Mauk, A. G. (1995) *Biochemistry 34*, 13895−13905.
23. Goodin, D. B., Davidson, M. G., Roe, J. A., Mauk, A. G., and Smith, M. (1991) *Biochemistry 30*, 4953−4961.
24. Tsaprailis, G., and English, A. M. (1996) *Can. J. Chem. 74*, 2250−2257.
25. Finzel, B. C., Poulos, T. L., and Kraut, J. (1984) *J. Biol. Chem. 259*, 13027−13036.
26. Smulevich, G., Wang, Y., Mauro, J. M., Wang, J., Fishel, L. A., Kraut, J., and Spiro, T. G. (1990) *Biochemistry 29*, 7174−7180.
27. Miller, V. P., DePillis, G. D., Ferrer, J. C., Mauk, A. G., and Ortiz de Montellano, P. R. (1992) *J. Biol. Chem. 267*, 8936−8942.
28. Smith, A. T., Sanders, S. A., Thorneley, R. N. F., Burke, J. F., and Bray, R. C. (1992) *Eur. J. Biochem. 207*, 507−519.
29. Meunier, B., Rodriguez-Lopez, J. N., Smith, A. T., Thorneley, R. N. F., and Rich, P. R. (1998) *Biochem. J. 330*, 303−309.
30. Ozaki, S., and Ortiz de Montellano, P. R. (1994) *J. Am. Chem. Soc. 116*, 4487−4488.
31. Ortiz de Montellano, P. R., Ozaki, S., Newmyer, S. L., Miller, V. P., and Hartmann, C. (1995) *Biochem. Soc. Trans. 23*, 223−227.
32. Welinder, K. G., and Andersen, M. B. (1993) Patent Appl. WO 93/24618.
33. Smulevich, G., Neri, F., Marzocchi, M. P., and Welinder, K. G. (1996) *Biochemistry 35*, 10576−10585.
34. Rasmussen, C. B., Hiner, A. N. P., Smith, A. T., and Welinder, K. G. (1998) *J. Biol. Chem. 273*, 2232−2240.
35. Smulevich, G., Feis, A., Focardi, C., and Welinder, K. G. (1994) *Biochemistry 33*, 15425−15432.
36. Choi, S., Spiro, T. G., Langry, K. C., Smith, K. M., Budd, D. L., and La Mar, G. N. (1982) *J. Am. Chem. Soc. 104*, 4345−4351.
37. Nissum, M., Neri, F., Mandelman, D., Poulos, T. L., and Smulevich, G. (1998) *Biochemistry 37*, 8080−8087.
38. Smulevich, G., Hu, S., Rodgers, K. R., Goodin, D. B., Smith, K. M., and Spiro, T. G. (1996) *Biospectroscopy 2*, 365−376.
39. Veitch, N. C., Gao, Y., and Welinder, K. G. (1996) *Biochemistry 35*, 14370−14380.
40. Neri, F., Kok, D., Miller, M. A., and Smulevich, G. (1997) *Biochemistry 36*, 8947−8953.
41. Welinder, K. G. (1992) *Curr. Opin. Struct. Biol. 2*, 388−394.
42. Edwards, S. L., and Poulos, T. L. (1990) *J. Biol. Chem. 265*, 2588−2595.
43. Erman, J. E. (1974) *Biochemistry 13*, 34−44.
44. Neri, F., Kok, D., Miller, M. A., and Smulevich, G. (1998) *Biochemistry 37*, 8268−8268.
45. Asher, S. A., Vickery, L. E., Schuster, T. M., and Sauer, K. (1977) *Biochemistry 16*, 5849−5856.
46. Asher, S. A., and Schuster, T. M. (1979) *Biochemistry 18*, 5377−5387.
47. Desbois, A., Lutz, M., and Banerjee, R. (1979) *Biochemistry 18*, 1510−1518.
48. Asher, S. A., and Schuster, T. M. (1981) *Biochemistry 20*, 1866−1873.
49. Asher, S. A., Adams, M. L., and Schuster, T. M. (1981) *Biochemistry 20*, 3339−3346.
50. Yu, N.-T. (1986) in *Methods in Enzymology* (Riordan, J. F., and Vallee, B. L., Eds.) Vol. 130, pp 350−409, Academic Press, New York.
51. Sitter, A. J., Shifflett, J. R., and Terner, J. (1988) *J. Biol. Chem. 263*, 13032−13038.
52. Feis, A., Marzocchi, M. P., Paoli, M., and Smulevich, G. (1994) *Biochemistry 33*, 4577−4583.
53. Kitagawa, T. (1988) in *Biological Applications of Raman Spectroscopy* (Spiro, T. G., Ed.) Vol. III, pp 97−131, Wiley and Sons, New York.
54. Kalsbeck, W. A., Ghosh, A., Pandey, R. K., Smith, K. M., and Bocian, D. F. (1995) *J. Am. Chem. Soc. 117*, 10959−10968.
55. Kunishima, N., Fukuyama, K., Matsubara, H., Hatanaka, H., Shibano, Y., and Amachi, T. (1994) *J. Mol. Biol. 235*, 331−344.
56. Erman, J. E., Vitello, L. B., Miller, M. A., Shaw, A., Brown, K. A., and Kraut, J. (1993) *Biochemistry 32*, 9798−9806.
57. DeLauder, S. F., Mauro, J. M., Poulos, T. L., Williams, J. C., and Schwartz, F. P. (1994) *Biochem. J. 302*, 437−442.
58. Andersen, M. B., Hsuanyu, Y., Welinder, K. G., Schneider, P., and Dunford, H. B. (1991) *Acta Chem. Scand. 45*, 206−211.
59. Andersen, M. B., Hsuanyu, Y., Welinder, K. G., Schneider, P., and Dunford, H. B. (1991) *Acta Chem. Scand. 45*, 1080−1086.
60. Sage, J. T., Morikis, D., and Champion, P. M. (1991) *Biochemistry 30*, 1228−1237.
61. Palanappian, V., and Bocian, D. F. (1994) *Biochemistry 33*, 14264−14274.
62. Smulevich, G., Paoli, M., De Sanctis, G., Mantini, A. R., Ascoli, F., and Coletta, M. (1997) *Biochemistry 36*, 640−649.
63. Creighton, T. E. (1993) *Proteins. Structures and Molecular Properties*, pp 16−17, W. H. Freeman and Co., New York.

BI982811+